J|A|C|S
ARTICLES
Published on Web 01/07/2006

Computational Insights into the Mechanism of Radical Generation in B_{12}-Dependent Methylmalonyl-CoA Mutase

Renata A. Kwiecien,[†] Ilja V. Khavrutskii,[‡,§] Djamaladdin G. Musaev,[‡] Keiji Morokuma,*[,‡] Ruma Banerjee,*[,||] and Piotr Paneth*[,†]

Contribution from the Institute of Applied Radiation Chemistry, Technical University of Lodz, Zeromskiego 116, 90-924 Lodz, Poland, Department of Chemistry and Cherry L. Emerson Center for Scientific Computation, Emory University, Atlanta, Georgia 30322, and Department of Biochemistry, The Beadle Center, University of Nebraska−Lincoln, Lincoln, Nebraska 68588-0664

Received September 22, 2005; E-mail: paneth@p.lodz.pl.; morokuma@chem.emory.edu.; rbanerjee@unl.edu

Abstract: ONIOM calculations have provided novel insights into the mechanism of homolytic Co−C5′ bond cleavage in the 5′-deoxyadenosylcobalamin cofactor catalyzed by methylmalonyl-CoA mutase. We have shown that it is a stepwise process in which conformational changes in the 5′-deoxyadenosine moiety precede the actual homolysis step. In the transition state structure for homolysis, the Co−C5′ bond elongates by ∼0.5 Å from the value found in the substrate-bound reactant complex. The overall barrier to homolysis is ∼10 kcal/mol, and the radical products are ∼2.5 kcal/mol less stable than the initial ternary complex of enzyme, substrate, and cofactor. The movement of the deoxyadenosine moiety during the homolysis step positions the resulting 5′-deoxyadenosyl radical for the subsequent hydrogen atom transfer from the substrate, methylmalonyl-CoA.

Introduction

Methylmalonyl-CoA mutase (MCM) is the only adenosylcobalamin (AdoCbl)-dependent enzyme that is found in mammals and catalyzes a radical-based transformation of methylmalonyl-CoA (MCA) to succinyl-CoA. The cofactor serves as a radical reservoir that generates the working 5′-deoxyadenosyl radical (dAdo•) via homolysis of the Co−C5′ bond to initiate the rearrangement reaction[1] (Figure 1). The mechanism by which the enzyme effects the observed $\sim 10^{12}$-fold rate acceleration of the homolysis step and propagates reactive organic radicals with high fidelity are important issues that remain to be fully elucidated. The observed rate constant for the homolysis reaction obtained from presteady-state kinetic studies is a composite of several steps that include substrate binding, conformational changes, and bond-forming/breaking reactions. Of these, only the effect of the substrate binding step can be readily deconvoluted by examining the substrate concentration dependence of the k_{obsd} for homolysis.[2] The remaining steps are spectroscopically silent and therefore experimentally relatively intractable. Computational studies offer an alternative and complementary approach for examining the mechanistically complex Co−C5′ homolysis step. However, the size of the corrin ring, the presence of a transition metal, and the radical nature of dAdo• combine to make computational studies on this system challenging. Recently, the homolysis step catalyzed by a related AdoCbl-dependent isomerase, glutamate mutase, has been reported.[3] In the present study, we have employed an ONIOM[4] approach that reveals the role of active site residues in stabilization of the radicals generated by homolytic rupture of the Co−C5′ bond.

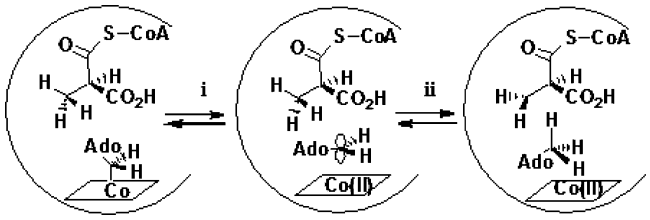

Figure 1. Presteady-state steps in the MCM-catalyzed reaction comprising formation of dAdo• (step i) and hydrogen atom transfer from the substrate to dAdo• (step ii).

Homolysis of the Co−C5' bond in the MCM-catalyzed reaction exhibits an unusual sensitivity to isotopic substitution in the substrate,[5] which has been interpreted as evidence for kinetic coupling of the first two steps illustrated in Figure 1.

[†] Technical University of Lodz.
[‡] Emory University.
[§] Present address: Department of Molecular Biology, Scripps Research Institute, La Jolla, CA.
[||] University of Nebraska-Lincoln.

(1) (a) Banerjee, R. *Chem. Rev.* **2003**, *103*, 2083. (b) Vlasie, M. D.; Banerjee, R. *J. Am. Chem. Soc.* **2003**, *125*, 5431.
(2) Chowdhury, S.; Banerjee, R. *Biochemistry* **2000**, *39*, 7998.
(3) Jensen, K. P.; Ryde, U. *J. Am. Chem. Soc.* **2005**, *127*, 9117.
(4) (a) Dapprich, S.; Komáromi, I.; Byun, K. S.; Morokuma, K.; Frisch, M.-J. *J. Mol. Struct. (THEOCHEM)* **1999**, *461*, 1. (b) Svensson, M.; Humbel, S.; Froese, R. D. J.; Matsubara, T.; Sieber, S.; Morokuma, K. *J. Phys. Chem.* **1996**, *100*, 19357. (c) Maseras, F.; Morokuma, K. *J. Comput. Chem.* **1995**, *16*, 1170. (d) Humbel, S.; Sieber, S.; Morokuma, K. *J. Chem. Phys.* **1996**, *105*, 1959. (e) Froese, R. D. J.; Humbel, S.; Svensson, M.; Morokuma, K. *J. Phys. Chem. A* **1997**, *101*, 227. (f) Svensson, M.; Humbel, S.; Morokuma, K. *J. Chem. Phys.* **1996**, *105*, 3654.

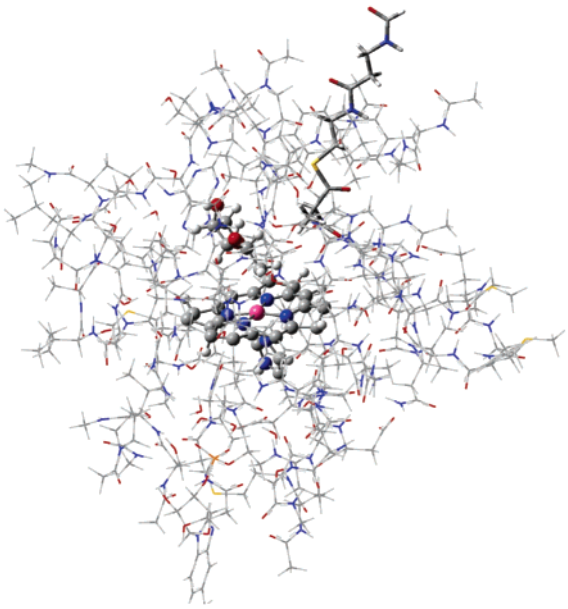

Figure 2. MCM active site in the 4REQ model. QM atoms are shown as spheres, MM atoms as sticks (MCA atoms are shown as tubes).

Theoretical studies on the homolysis step[6] revealed that small models comprising only the Corrin ring and the two axial ligands are insufficient to model the reaction and that inclusion of some active site amino acids is essential for stabilization of the intermediates. In this study, we have used three models of the MCM active site to probe the energetics and geometrical features of the homolysis step. The 4req model shown in Figure 2 is based on the crystal structure 4REQ[7] deposited in the Protein Data Bank (PDB) and corresponds to the closed and reactive conformation of the enzyme. It contains the reactant, methylmalonyl-CoA, bound to the active site, the cofactor, and all amino acids within a 15 Å radius from the cobalt atom. Truncated AdoCbl and the imidazole ring of its lower ligand are shown in ball-and-stick rendering. This latter part was treated quantum mechanically in ONIOM calculations (the QM part). It was also used as an additional model devoid of the contributions of the enzymatic environment. Following the literature,[3] it is denoted as a vacuum model. The second model, denoted 4req−mca, is based on 4REQ, but the reactant is subtracted out. In the 4REQ structure, the Co−C5′ bond of AdoCbl is cleaved. The third model, denoted 3req, represents the unreactive, open conformation of MCM and is based on the 3REQ[7] crystal structure. It lacks the substrate molecule, and the Co−C5′ bond is intact. It was anticipated that comparison of the 4req and the 4req−mca models would allow evaluation of the influence of the substrate on the homolysis step. On the other hand, comparison of the 4req and 3req models would furnish insights into the substrate-induced conformational change on catalysis of the homolytic cleavage step.

Materials and Methods

As described in the Introduction, calculations were carried out on models that were based on two crystal structures deposited in the Protein Data Bank (PDB) of the closed, reactive (4REQ) and the open, unreactive (3REQ) forms of MCM. Each model included all amino acids within 15 Å from the cobalt atom of AdoCbl, resulting in 1372, 1339, and 1276 atoms in 4req, 4req−mca, and 3req models, respectively. The 4req model, built in this way, contained the following amino acids: Tyr89, Ala116, Phe117, Asp118, Leu119, Pro120, Thr121, His122, Met138, Ala139, Thr166, Glu203, Phe204, Met205, Val206, Arg207, Asn208, Thr209, Tyr243, His244, Met245, Gln246, Glu247, Ala248, Phe287, Gln330, Thr331, Ser332, Gly333, Trp334, Ser335, Leu336, His364, Thr365, Asn366, Ser367, Leu368, Asp369, Glu370, Ala371, Ile372, Ala373, Leu374, Pro375, Lys604, Met605, Gly606, Gln607, Asp608, Gly609, Hsp610, Asp611, Arg612, Gly613, Ser656, Leu657, Ala658, Gly659, Gly686, Val687, and Pro707. The 3req model that corresponds to a different conformation of MCM includes the same amino acids but is missing the water molecules present in the 4REQ structure. The N- and C-termini of each model were capped with NHMe and C(O)Me moieties, respectively, where protein chains were truncated. The quantum mechanical part (QM) in all models was comprised of 71 atoms including the corrin ring without side chains, ribose as the upper ligand, and imidazole as the lower ligand. The remaining part of the cofactor, the reactant in the case of the 4req model, and the active site residues were included in the MM part of the model. The substrate was truncated at the 15 Å boundary of the model. Valences of the QM part were complemented by the hydrogen-like link atoms[8] in places where a covalent bond separated the QM part from the MM part. Cartesian coordinates of heavy atoms of the capping NHMe and C(O)Me moieties were fixed at their crystallographically determined positions during optimizations.

Relaxed potential energy scan (PES) calculations along the Co−C5′ bond were carried out using the ONIOM protocol as implemented in Gaussian 03[9] with the default convergence criteria and a step size of 0.15 Å starting from the fully optimized structure. The energy and gradients of the QM part were computed externally using a spin unrestricted procedure[10] with the BP86 functional,[11] def-SV(P) basis set,[12] and resolution of the identity (RI) method[13] in an auxiliary basis set for the Coulombic long-range energy component as implemented in Turbomole.[14] The MM part was treated using the Amber force field.[15] Amber parameters for vitamin B_{12} were taken from the literature.[16] Missing parameters were generated on the basis of B3LYP/6-31G(d) optimization[17] of the truncated substrate and are provided in the Supporting Information.

A search for the transition state was performed on the basis of two structures of the PES scan of the 4req model. Finding transition states

(5) Padmakumar, R.; Padmakumar, R.; Banerjee, R. *Biochemistry* **1997**, *36*, 3713.
(6) (a) Kozlowski, P. M. *Curr. Opinion Chem. Biol.* **2001**, *5*, 736. (b) Andruniow, T.; Zgierski, M. Z.; Kozlowski, P. M. *J. Am. Chem. Soc.* **2001**, *123*, 2679. (c) Jensen, K. P.; Ryde, U. *J. Phys. Chem. A* **2003**, *107*, 7539. (d) Dölker, N.; Maseras, F.; Lledos, A. *J. Phys. Chem. B* **2001**, *105*, 7564. (e) Freindorf, M.; Kozlowski, P. M. *J. Am. Chem. Soc.* **2004**, *126*, 1928. (f) Dölker, N.; Maseras, F.; Siegbahn, P. E. M. *Chem. Phys Lett.* **2004**, *386*, 174.
(7) Mancia, F.; Evans, P. R. *Structure* **1998**, *6*, 711.
(8) Singh, U.; Kollman, P. *J. Comput. Chem.* **1986**, *7*, 718.
(9) Frisch, M. J. et al. *Gaussian 03*, Development version; Gaussian, Inc.: Pittsburgh, PA, 2003.
(10) Pople, J. A.; Nesbet, R. K. *J. Chem. Phys.* **1954**, *22*, 571.
(11) (a) Becke, A. D. *Phys. Rev. A* **1988**, *38*, 3098. (b) Perdew, J. P. *Phys. Rev. B* **1986**, *33*, 8822.
(12) Schaefer, A.; Horn, H.; Ahlrichs, R. *J. Chem. Phys.* **1992**, *97*, 2571.
(13) (a) Eichkorn, K.; Treutler, O.; Öhm, H.; Häser, M.; Alrichs, R. *Chem. Phys. Lett.* **1995**, *242*, 652. (b) Eichkorn, K.; Weigend, F.; Treutler, O.; Alrichs, R. *Theor. Chem. Acc.* **1997**, *97*, 119. (c) Alrichs, R.; Elliot, S.; Huniar, U. *Ab Initio Treatment of Large Molecules in Modern Methods and Algorithms of Quantum Chemistry, Proceedings*, 2nd ed.; Grotendorst, J., Ed.; John von Neumann Institute for Computing: Jülich, NIC Series 3, 2000; p 7.
(14) (a) Alrichs, R.; Bär, M.; Häser, M.; Horn, H.; Kölmel, C. *Chem. Phys. Lett.* **1989**, *162*, 165. (b) Karlsruhe Quantum Chemistry Group http://www.turbomole.com; accessed 2002.
(15) (a) Cornell, W. D.; Cieplak, P.; Bayly, C. I.; Gould, I. R.; Merz, K. M., Jr.; Ferguson, D. M.; Spellmeyer, D. C.; Fox, T.; Caldwell, J. W.; Kollman, P. A. *J. Am. Chem. Soc.* **1995**, *117*, 5179.
(16) (a) Marques, H. M.; Ngoma, B.; Egan, T. J.; Brown, K. L. *J. Mol. Struct.* **2001**, *561*, 71. (b) Marques, H. M.; Brown, K. L. *J. Mol. Struct. (THEOCHEM)* **1995**, *340*, 97.
(17) (a) Becke, A. D. *J. Chem. Phys.* **1993**, *98*, 5648. (b) Stephens, P. J.; Devlin, F. J.; Chablowski, C. F.; Frisch, M. J. *J. Phys. Chem.* **1994**, *98*, 11623. (c) Ditchfield, R.; Hehre, W. J.; Pople, J. A. *J. Chem. Phys.* **1971**, *54*, 724. (d) Hehre, W. J.; Ditchfield, R.; Pople, J. A. *J. Chem. Phys.* **1972**, *56*, 2257.

Table 1. Selected Dihedral Angles (deg) of dAdo as Functions of the Co−C5′ Distance (Å)

	4req				4req-mca				3req				vacuum		
Co−C5	χ_{CN}	θ_0	P	θ_m	χ_{CN}	θ_0	P	θ_m	χ_{CN}	θ_0	P	θ_m	θ_0	P	θ_m
2.0	62.4	2.6	86.6	43.5					155.8	31.4	338.7	33.7			
2.15	63.0	1.8	87.6	42.9	60.3	5.9	81.8	41.4	155.8	31.0	333.9	34.5	30.3	46.5	44.0
2.3	63.5	1.4	88.1	42.2	60.9	7.0	80.1	40.7	155.8	30.7	330.5	35.3	30.4	46.6	44.2
2.45	63.5	1.0	88.6	41.5	61.4	8.3	78.0	39.8	155.9	30.3	327.4	36.0	31.2	45.1	44.2
2.6	64.0	1.8	87.5	41.0	62.5	10.3	74.3	38.2	155.6	30.2	325.0	36.9	31.3	44.6	44.0
2.75	64.4	3.1	85.6	40.4	63.8	12.8	69.1	36.7	155.5	30.1	322.8	37.8	29.7	48.1	44.5
2.9	64.7	4.1	83.6	36.8	65.3	16.1	62.6	35.2	155.1	29.9	320.8	38.6	29.8	48.0	44.6
3.05	54.7	27.8	355.5	27.9	71.2	29.0	33.8	35.0	154.3	29.7	318.7	39.6	30.2	47.1	44.4
3.2	55.4	28.7	356.4	28.8	72.2	31.4	29.2	36.0	153.7	29.4	316.9	40.3	30.6	46.1	44.1

in large systems is not trivial. Geometry optimization methods that are generally used for large systems, studied with MM or semiempirical methods, require many energy and gradient evaluations and can only search for minima. Methods that are generally used for smaller systems, studied with QM methods, require fewer optimization cycles and can search for saddle points but cannot be used for the current system because the computational time scales cubically with the size of the system. As an alternative to these conventional optimizers, one can use a hybrid optimizer for QM/MM potential surfaces,[18] which performs much better than any of the conventional geometry optimization schemes. Details of the optimization routines used herein are given elsewhere.[19] In PES calculations and in optimizations of stationary points, default Gaussian convergence criteria were tightened by a factor of 10, to ascertain the convergence of floppy motions.

Results and Discussion

Initial points for the PES calculations were obtained by the closed-shell ONIOM(RI-BP86/def-SV(P):Amber) optimization of the models described under Materials and Methods. In the case of the 4REQ model, the corresponding 4REQ crystal structure contains a cofactor in which the Co−C5′ bond has been ruptured. This optimization results in the reformation of the Co−C5′ bond with a distance of 2.029 Å. We will refer to this point as structure **S**. Starting from this initial point, the Co−C5′ bond was elongated from 2.0 to 3.2 Å, and the remainder of the geometrical parameters was reoptimized; the resultant potential energy profiles are presented in Figure 3. The vacuum model (squares in Figure 3) of the cofactor alone shows a smooth energy increase that reaches a maximum at ∼26 kcal/mol at a Co−C5′ distance of ∼3.2 Å, in excellent agreement with recent results of Jensen and Ryde.[3] Similar results are obtained for the 3req model of the open, unreactive conformation of the enzyme. The energy difference between PES results for the 3req and vacuum models correlates well with the conformational differences in the ribose ring, for which a few kcal/mol difference in the relative stabilities is expected for the corresponding structures.[9]

For the 4req−mca, a small stabilization of the forming radical pair can be seen in agreement with earlier observations.[6] Note that the 4req−mca model represents a state that is not accessible experimentally since the conformational switch from the unreactive (3REQ) to the reactive (4REQ) conformation is triggered by substrate binding. The potential energy profiles indicate that the barrier for homolysis in the active conformation (the 4req−mca model) is substantially lower than in either the gas phase (the vacuum model) or the active site of the unreactive conformation (the 3req model). Thus, the conformational switch elicited by substrate binding is responsible for lowering the barrier for homolysis by >10 kcal/mol.

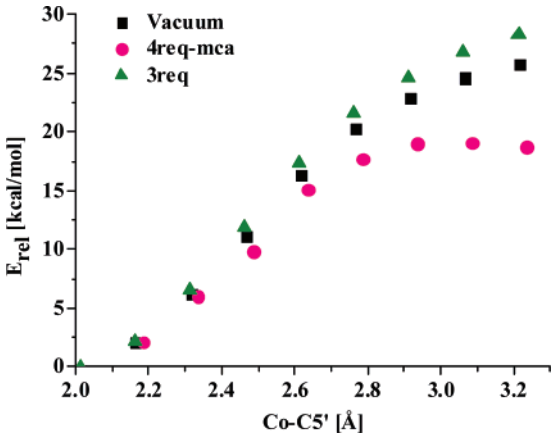

Figure 3. Potential energy profiles obtained by relaxed scans along the Co−C5′ bond for models without the MCA substrate.

The most interesting model is of course the 4req model, which corresponds to the closed and reactive state of the enzyme. Initial changes in the PES points up to ∼3 Å of the 4req−mca and 4req (data not shown) models are identical, but upon reaching a maximum on the PES, the 4req model shows a discontinuity in the energy profile that indicates that the Co−C5′ bond length solely is not a good approximation of the reaction coordinate for homolysis. This change in energy is paralleled by a concomitant and dramatic change in the conformation of the dAdo moiety. Thus, before discussing other effects accompanying elongation of the Co−C5′ distance, we turn our attention to conformational changes in dAdo.

Table 1 lists the conformational parameters of adenosine at discrete points on the relaxed potential energy scans. Parameters P (pseudorotation phase) and θ_m (amplitude) correspond to conformational analysis terminology introduced by Altona and Sundaralingam[20] and characterize the ribose puckering.[21] The dihedral angle χ_{CN} describes the adenine plane relative to the sugar ring and is defined by O1′−C1′−N9−C8, while θ_0 (C1′−C2′−C3′−C4′) describes the ribose ring (atom numbering is given in Figure 4). Note that the first (nominal) Co−C5′ distance

(18) (a) Maseras, F.; Morokuma, K. *J. Comput. Chem.* **1995**, *16*, 1170. (b) Vreven, T.; Morokuma, K.; Farkas, Ö; Schlegel, H. B.; Frisch, M. J. *J. Comput. Chem.* **2003**, *24*, 760. (c) Moliner, V.; Turner, A. J.; Williams, I. H. *Chem. Commun.* **1997**, 1271. (d) Turner, A. J.; Moliner, V.; Williams, I. H. *Phys. Chem. Chem. Phys.* **1999**, *1*, 1323. (e) Monard, G.; Prat-Resina, X.; Gonzalez-Lafont, A.; Lluch, J. M. *Int. J. Quantum Chem.* **2003**, *93*, 297. (f) Prat-Resina, X.; Bofill, J. M.; Gonzalez-Lafont, A.; Lluch, J. M. *Int. J. Quantum Chem.* **2004**, *98*, 367.
(19) Vreven, T.; Frisch, M. J.; Kudin, K. N.; Schlegel, H. B.; Morokuma, K. *Mol. Phys.* **2005**, in press.
(20) Altona, C.; Sundaralingam, M. *J. Am. Chem. Soc.* **1972**, *94*, 8205.
(21) Khoroshun, D. V.; Warncke, K.; Ke, S.-C.; Musaev, D. G.; Morokuma, K. *J. Am. Chem. Soc.* **2003**, *125*, 570.

Table 2. Selected Parameters Describing the Reactant Complex, Intermediate, Transition State, and Product for the 4req Model

structure	Co–C5 (Å)	E_{rel} (kcal/ mol)	χ_{CN} (deg)	θ_0 (deg)	P (deg)	θ_m (deg)	Co–N_{His610} (Å)	C5–$C_{do\ nor}$ (Å)	ω(av) (deg)
S	2.03	0	62.4	2.6	86.6	43.5	2.258	4.084	10.0
I	2.19	7.0	53.9	22.7	341.1	24.0	2.895	4.037	14.0
TS	2.67	10.1	53.3	26.0	351.5	26.3	2.497	3.777	11.5
P	4.29	2.5	58.5	34.5	12.2	35.2	2.222	3.226	10.5

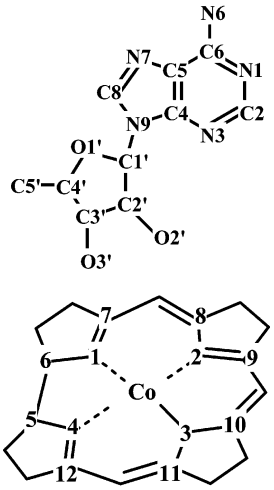

Figure 4. Atom numbering of AdoCbl used in this study.

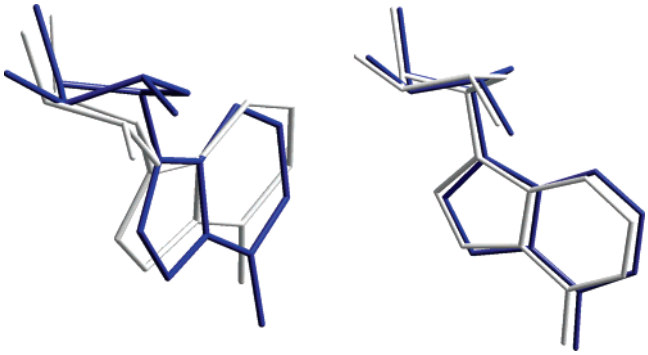

Figure 5. Conformations of dAdo along the PES. Left: 4req−mca model. Right: 3req model. Gray structures correspond to initial PES points. Structures in blue correspond to endpoints of the PES. Hydrogen atoms are omitted for clarity.

of 2.0 Å in Table 1 actually denotes the equilibrium value for **S**; 2.029 Å for the 4req, 4req−mca, and vacuum models; and 2.013 Å for the 3req model; all subsequent Co−C5′ distances in Table 1 represent increments of 0.15 Å from these values.

In the crystal structure 4REQ, the sugar ring is in the C2′-exo conformation, and the ONIOM (RI-BP86/def-SV(P):Amber) optimization of the 3req model starting from this initial structure preserved this conformation, yielding θ_0 equal to 31.4° at the optimized Co−C5′ bond distance of 2.013 Å (Table 1). The dAdo• part of the 3req model differs from the other models also in the conformation of the adenine. The adenine plane relative to the sugar ring, the χ_{CN} dihedral angle, is ∼90° larger in 3req than in the other models and is in a syn conformation. The ribose ring in the 3REQ model is in the C1′-endo, C2′-exo conformation. The conformation of dAdo does not change along the PES for the 3req model. This is illustrated by the structures on the right side of Figure 5. Blue structures show the endpoints of the PES, whereas gray ones indicate the corresponding starting points.

In contrast, in the reactive and closed 4req model in the initial

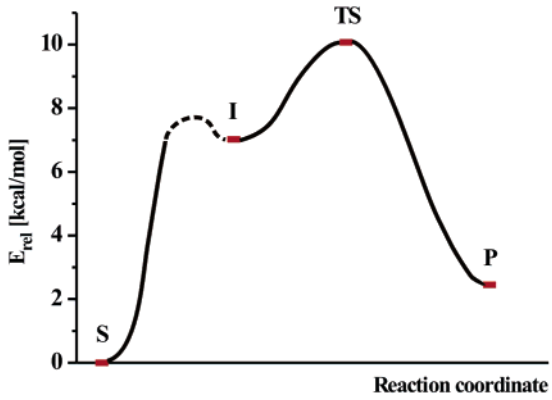

Figure 6. Energies of the stationary points along the PES for the homolysis of the Co−C5′ bond in MCM calculated for the 4req model.

state **S**, the ribose ring is in the O1′-endo conformation that is characterized by coplanarity of all four carbon atoms of the ring; the dihedral angle θ_0 for this initial structure is 2.6°. This conformation does not change significantly until the Co−C5′ bond reaches about 3 Å when it changes to C2′-exo with a θ_0 of about 28°. These changes are illustrated by the superimposed structures of the initial and final points on the 4req PES on the left side of Figure 5.

Changes mentioned previously in the dAdo conformation cause PES discontinuity for the 4req model around the maximum energy. This indicates that the cobalt−carbon bond alone becomes inadequate as the reaction coordinate in the region of greatest interest and that the glycosidic bond of dAdo also needs to be included. Since the adenine moiety in all models is treated at the MM (Amber) level, a special treatment has been used as discussed in the Materials and Methods section that was directed toward the search for the true transition state. This search was started from the points on the 4req PES that encompass the maximum energy point and the discontinuity point. We succeeded in finding the transition state for the homolysis step (referred to as **TS** in the following discussion) and confirmed that there is only one negative Hessian element and that it corresponds to the normal mode of Co−C5′ bond breaking. It is worth noting that this is the first time the convergence to the transition state of AdoCbl homolysis has been achieved despite numerous previous attempts.[6] The intrinsic reaction coordinate (IRC) calculations confirmed this assignment and revealed that the product (labeled **P**) is the radical pair that results from homolysis. On the reactant side of the IRC path, we reached a stationary point, which we refer to as the intermediate (**I**), which differs from the initial structure **S** in the dAdo conformation. The geometric features of all the stationary points for the 4req model are compiled in Table 2.

Energetically, the intermediate **I** is ∼7 kcal/mol higher in energy than the initial ternary enzyme complex **S** (Figure 6). We were unable to locate the transition state between **S** and **I**. This is because the potential energy surface is very flat in this area, which makes it very difficult to reach convergence.

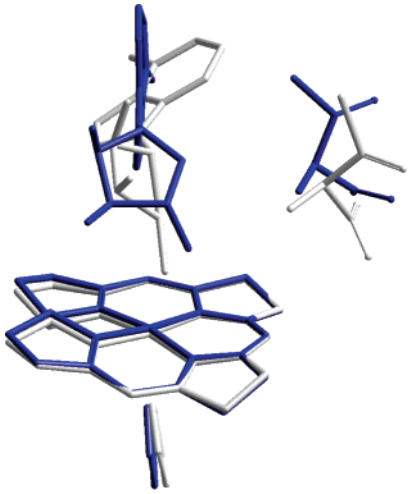

Figure 7. Overlay of the QM part with a MCA fragment of the initially optimized 4req structure (gray) with the **TS** structure (blue).

However, the fact that the surface is flat implies that the barrier is small, and we thus assume that the step from **S** to **I** is kinetically silent in the overall conversion between the **S** and **P** states. The subsequent homolysis is characterized by a very small energy barrier of ~3 kcal/mol and is exothermic by ~7.5 kcal/mol. Thus, overall, the homolysis step has a barrier of ~10 kcal/mol and is endothermic by ~2.5 kcal/mol.

We are now able to discuss geometric features of the stationary points for the 4req model(i.e., the model for Co−C5′ homolysis in MCM). The conformation of the adenine ring in the models derived from the 4REQ crystal structure is anti in the Pullman notation,[22] while, as mentioned earlier, the corresponding structure in the 3req model is syn. Initially, the major change in the 4req model is in the ribose conformation switching from O1′-endo in **S** to the C2′-exo in **I**, which is paralleled by a small Co−C5′ bond elongation from 2.03 to 2.19 Å. Upon reaching **I**, the dAdo conformation does not change significantly in the subsequent conversion to **P** via **TS**. The transition from **S** to **I** results in loosening the interactions between the corrin ring and its lower ligand, His610. This loosening is accompanied by small changes of the corrin ring conformation that is reflected in the fold angle[23] ω(av) that is an average of eight selected dihedral angles, which describe the corrin ring planarity. The increase in the fold angle by about 4° indicates that the corrin ring becomes more folded. The changes, however, are minimal and disappear on the subsequent transition from **I** to **TS** to **P**, and the Co−His610 distance returns to its original value. These changes in the fold angle and the Co−His610 distance correspond to the butterfly motion of the corrin ring that has been postulated previously as being important for inducing homolysis.[24] Starting from the intermediate **I**, the ribose ring continues its conformational change with θ_0 reaching ~30° characteristic for the dissociated dAdo moiety, while the relative ribose−adenine rotation described by χ_{CN} reaches a minimum at the **TS** and then goes up again toward the initial value of ~60°. This substantial repositioning of the adenine ring of dAdo between the **S** and the **TS** states as illustrated in Figure 7 is different from the situation in glutamate mutase where the conformational change is apparently restricted to a pseudorotation in the ribose ring and the adenine ring remains fixed.[25]

Table 3. Hydrogen Bonding Network at the Stationary Points of 4req Model[a]

donor	acceptor	S	I	TS	P
Arg207	MCA(CO_2^-)	2.102			
Arg207	MCA(CO_2^-)	1.805	1.858	1.875	2.069
Arg207	corrin(C(O)NH_2)		2.443	2.400	2.100
His244	MCA(CO_2^-)	2.153	1.695	1.694	1.686
His244	MCA(C=O)	1.998			
Tyr89	MCA(CO_2^-)	1.764	1.871	1.839	1.704
H_2O170	Tyr89	1.759	1.800	1.797	1.789
Phe117(amid)	H_2O170				2.286
Tyr243	Thr331(amid)	1.697	1.677	1.677	1.680
H_2O576	Tyr243	2.088			
H_2O576	dAdo(3′-OH)		1.916	1.894	1.865

[a] H−acceptor distances are given in angstroms.

An important outcome of the conformational rearrangement of the dAdo moiety is that it poises the resulting dAdo• for the subsequent step in the reaction. Thus, the distance between the hydrogen atom acceptor (i.e., the C5′ atom of dAdo•) and the hydrogen atom donor (i.e., the methyl carbon (C_{donor}) of methylmalonyl-CoA) diminishes from the initial value of ~4.1 to 3.8 Å in the **TS** and to 3.2 Å in the product. Figure 7 includes a fragment of MCA to illustrate this change between **S** and **TS**.

Finally, changes in the hydrogen bond network (Table 3) within the active site deserve discussion. On the basis of the empirical rules developed by McDonald and Thornton[26] to study hydrogen bonds in proteins (D−A < 3.9 Å, H−A < 2.5 Å, D−H−A > 90.0°, AA−A−D > 90.0°, and AA−A−H > 90.0°, where A is the proton acceptor and D the proton donor), we identified atoms, which may participate in stabilization of catalytic intermediates in MCM. Initially, methylmalonyl-CoA is held in place by a bifurcated hydrogen bond between the oxygen atoms of the carboxyl group of the substrate and Arg207 and the carbonyl oxygen and His244. However, with the progress of the Co−C5′ bond breakage, the bond to His244 and one of the bonds to Arg207 are ruptured. Arg207 forms a new hydrogen bond with an amide sidearm of the corrin ring, which becomes shorter by 0.34 Å in **P**. The other bond to Arg207 gradually weakens and is shorter by about 0.26 Å in the transition state. The other amino acid that is involved in hydrogen bonding of the substrate is Tyr89. It experiences a major movement upon substrate binding. However, during conversion from **S** to **P** this bond, as well as its bonding to crystallographic water, undergoes only minor changes. The second crystallographic water, H_2O576, is initially held in position by Tyr243 but during progress of the reaction loses its contact with this amino acid and forms a strong hydrogen bond to the 3′-hydroxyl group of dAdo.

Conclusions

We have shown that homolysis of AdoCbl catalyzed by MCM is a stepwise but kinetically silent process in which conformational changes in dAdo and concomitant changes in the electrostatic interactions between active site residues, cofactor, and substrate are in a preequilibrium step that precede the actual homolysis step. These conformational changes cause the Co−

(22) Pullman, B.; Saran, A. *Prog. Nucleic Acid Res. Mol. Biol.* **1976**, *18*, 215.
(23) Jensen, K. P.; Sauer, S. P. A.; Liljefors, T.; Norrby, P.-O. *Organometallics* **2001**, *20*, 550.
(24) Kozlowski, P. M.; Zgierski, M. Z. *J. Phys. Chem. B* **2004**, *108*, 14163.
(25) Gruber, K.; Reitzer, R.; Kratky, C. *Angew. Chem., Int. Ed.* **2001**, *40*, 3377.
(26) McDonald, I. K.; Thornton, J. M. *J. Mol. Biol.* **1994**, *238*, 777.

C5′ bond to elongate by ∼0.16 Å and destabilizes AdoCbl by ∼7 kcal/mol. The transition state structure for homolysis showed that the Co−C5′ bond elongates by ∼0.5 Å between the substrate−enzyme complex and the transition state. The radical products of the homolysis are ∼2.5 kcal/mol less stable than the initial ternary complex of enzyme, substrate, and cofactor and geometrically poised for the subsequent hydrogen atom transfer step. Inclusion of the active site environment is required for simulating the energy profile of Co−C5′ bond homolysis in MCM. The size of the resulting model presents challenges that could be handled by the ONIOM approach. This study computes the role of active site residues in stabilization of the radicals in the MCM-catalyzed reaction and suggests a possible pathway for the forward propagation of the cofactor radical to the substrate.

Acknowledgment. This work was supported by grants from the NIH (5R03TW001212 to R.B. and P.P. and DK45776 to R.B.), State Committee for Scientific Research, Poland 3 T09A 028 26 (P.P.), and NSF CHE-0209660 and AFOSR DURIP FA9550-04-1-0321 (K.M. and D.G.M.). We thank Dr. Stephan Irle for helpful discussions on the computational methodology.

Supporting Information Available: Amber parameters used for the model of MCM, energies, and coordinates of the **S** and **TS** states, as well as complete ref 9. This material is available free of charge via the Internet at http://pubs.acs.org.

JA056333J